Aerial Surveillance System with Multiple Agents for Moving Targets

Satoshi HOSHINO[1†], Takeshi KATSUMOTO[2], Shigemichi SAITOH[1], Naoaki ITABASHI[2], Tomoki KABAYAMA[2], and Mitsuru KONO[2]

[1]Department of Mechanical and Intelligent Engineering Graduate School of Engineering Utsunomiya University, Japan
(Tel: +81-28-689-6053; E-mail: hosino@cc.utsunomiya-u.ac.jp)
[2]SUBARU Inc., Japan

Abstract: In this paper, we focus on an aerial surveillance system composed of multiple agents, such as sentinels and searchers. In the surveillance system, single sentinel detects a position of an incoming target, and multiple searchers approach and identify the target. In order for the searchers to identify moving targets as many as possible, it is required to optimize the approach behavior in consideration of the future positions. For these challenges, we use a directional statistics and value iteration method. Through simulation experiments, we show that the surveillance system is able to estimate the future positions of a target. We further show that the searchers based on the optimized approach behavior identify the most moving targets. Finally, we discuss the effectiveness of the surveillance system for the moving targets.

Keywords: Aerial Surveillance, Multi-Agent Systems, Directional Statistics, Bayes' Theorem, Optimization.

1. INTRODUCTION

In this paper, we focus on an aerial surveillance system composed of multiple agents, such as unmanned aerial vehicles, UAVs. Compared to ground vehicles, the aerial agents are capable of monitoring broader area. Basilico *et al.* have presented an aerial surveillance system composed of two types of UAVs [1]. **Fig. 1** illustrates the surveillance system.

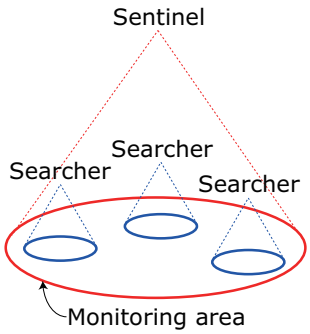

Fig. 1 Aerial surveillance system composed of sentinel and searchers

As the UAVs, single sentinel and multiple searchers are used. The sentinel operates at a place higher than the searchers. A monitoring area of the sentinel is drawn by a red circle. If an unidentified event occurs in the area, the sentinel detects the position. However, the sentinel is not capable of identifying the event precisely. On the other hand, the searcher is able to identify the event in the sensing range drawn by a blue circle. Therefore, these heterogeneous multi-agents played different roles in the surveillance system.

Basilico *et al.* have succeeded in identifying events by dispatching the searchers to the events detected by the sentinel. However, fixed events, e.g., wildfires, have been assumed. On the other hand, we assume moving targets, such as animals, in this paper.

† Satoshi HOSHINO is the presenter of this paper.

In our surveillance system, one sentinel and multiple searchers are used as illustrated in Fig. 1. The sentinel hovers in the same place, and the searchers move to approach targets. In order for the searchers to identify moving targets as many as possible, it is required to solve the following challenges:

1. estimate the future positions of a target and
2. approach the target efficiently.

For the first challenge, we use a directional statistics. The target motion monitored by the sentinel is quantified on the basis of von Mises circular distribution in Section 2. The von Mises distribution expresses the moving direction of a target. In Section 3, we estimate the future positions of the target with the use of the von Mises distribution. For this purpose, a moving probability of the target is calculated on the basis of Bayes' theorem. For the second challenge, we optimize the approach behavior of searchers toward the target in Section 4. For this purpose, we use a value iteration method and present two reward functions focusing on the moving probability.

Through simulation experiments, we show that the surveillance system is able to estimate the future positions of a target. We further show that the searchers based on the optimized approach behavior identify the most moving targets. Finally in Section 6, we discuss the effectiveness of the surveillance system for the moving targets.

2. MOVING DIRECTION OF TARGET

For a moving target, Best *et al.* have proposed a trajectory prediction method in an indoor environment [2]. Since the moving direction of a target is restricted by the environmental layout, they succeeded in predicting the future trajectory by assuming destinations. On the other hand, the aerial environment does not have a layout. Hence, the moving direction is not restricted. As a result, it is impossible to predict the moving direction.

For this problem, we use a directional statistics. The target motion monitored by the sentinel is quantitatively

expressed on the basis of the von Mises distribution. The von Mises distribution has a circular shape. Thus the probability density is defined along the circle of a monitoring area. **Fig. 2** shows a top view of the monitoring area. In the surveillance system, the monitoring area is divided into cells.

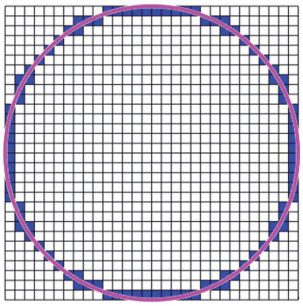

Fig. 2 Top view of circular monitoring area of sentinel divided into cells

The circle indicates the monitoring area of a sentinel. The sentinel detects the position of an incoming target. The target moves toward a destination. The blue cells corresponding to the edge of the monitoring area are candidates for the destinations. From these candidate cells, the target selects a destination. The destination cell is unknown to the system, i.e., sentinel and searchers.

The von Mises distribution is based on the target motion. The target motion is monitored by the sentinel. Hence, the moving direction of the target is expressed by the probability density function of the von Mises distribution as follows:

$$f(\mu, \theta) = \frac{\exp\{\beta \cos(\theta - \mu)\}}{2\pi I_0(\beta)}, \tag{1}$$

where β is a statistical direction. This parameter represents a measure of concentration on the moving direction. I_0 represents the modified Bessel function of order 0. μ and θ are angle parameters defined in the 2D space, (x, y), as illustrated in **Fig. 3**.

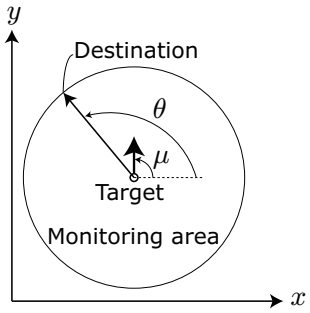

Fig. 3 Angle parameters μ and θ

The circle denotes the monitoring area. The target moves in the direction parallel to the axis of y. For this moving direction, μ, the probability density of the von Mises distribution, given a destination to each of the candidate cells depending on θ, is derived as shown in **Fig. 4**.

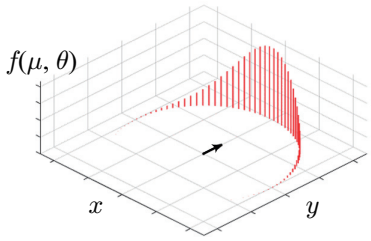

Fig. 4 Example of von Mises distribution ($\beta = 5$, $\mu = 0$)

The target is moving in the direction of $\mu = 0$ indicated by the arrowed line. For each of the candidate cells, the probability density is drawn by a red bar. The shape of the von Mises distribution becomes sharp and the probability densities of the candidate cells in the moving direction are increased as β increases. On the other hand, the shape of the distribution becomes smooth as β decreases.

β in Eq. (1) is derivable from a statistical direction of the moving target [3]. As well as our previous work, we derive β by using the Newton-Raphson method. For this purpose, we define the statistical direction as follows:

$$\frac{I_1(\beta)}{I_0(\beta)} = \frac{1}{N} \sum_{n=1}^{N} \cos(\mu_n - \mu_a), \tag{2}$$

where $I_1(\cdot)$ represents the modified Bessel function of order 1. μ_n is a moving direction of the target in n-th monitoring step as illustrated in **Fig. 5**. The sentinel continues to monitor the moving direction, μ_n, of the target in each time step.

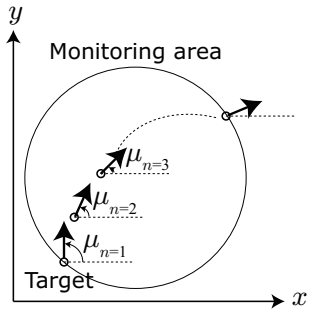

Fig. 5 Monitored moving direction of target

From the N directional data, μ_a in Eq. (2) is calculated as $\mu_a = \tan^{-1} \frac{\sum_{n=1}^{N} \sin(\mu_n)}{\sum_{n=1}^{N} \cos(\mu_n)}$. While μ_n indicates the moving direction at that position, μ_a indicates the moving direction based on the entire data N. Therefore, β is increased as a target moves in a linear manner. In this case, the target is expected to continue moving in the same direction. On the other hand, β is decreased as a target moves in different directions. In this case, since the probability densities of all the candidate cells become uniform, the target is expected to move in any direction.

3. FUTURE POSITIONS OF TARGET

Each time a target is monitored, the probability density of the von Mises distribution, f, is calculated from Eq.

(1). The probability densities in the candidate cells (see blue ones in Fig. 2) are used for estimating the future positions of the target. For an unknown destination of the target, we assume a destination cell, θ_η. At time t, the current position of the target is represented by x_t. The moving probability of the target from x_t to X_{t+1} at time $t+1$ is formulated as follows:

$$P(X_{t+1}|x_t,\theta_\eta) = K^{-1}\exp[-\alpha\{\delta(x_t,X_{t+1},\theta_\eta) - \delta(x_t,\theta_\eta)\}] \times f(\mu,\theta), \quad (3)$$

where the normalizing constant, K, is defined as $K = \sum_{x_{t+1}\in\chi^+} Pr(X_{t+1}|x_t,\theta_\eta)$. $\delta(\cdot)$ represents a distance composed of the parameters. Thus $\delta(x_t,X_{t+1},\theta_\eta) = \delta(x_t,X_{t+1}) + \delta(X_{t+1},\theta_\eta)$, where $\delta(A,B)$ represents an Euclidean distance between A and B. χ^+ is a set of x_{t+1}, which is a reachable position from the current position, x_t, in one step.

Eq. (3) is based on a probabilistic dynamics model [2]. As can be seen in the last factor, the probability density function is additionally used in this model. As a result, the moving probability of the target is calculated in consideration of the moving direction even in the aerial environment. In each cell, the moving probability of the target at time t is formulated as follows:

$$P(X_{t+1}|x_{1:t}) = \sum_{\theta_\eta\in\Theta}[P(X_{t+1}|x_t,\theta_\eta) \times P(\theta_\eta|x_{1:t})], \quad (4)$$

where x_1 represents a position when the target was firstly monitored by the sentinel. Θ represents a set of the candidate cells for a destination. $P(X_{t+1}|x_t,\theta_\eta)$ is derived directly from Eq. (3). $P(\theta_\eta|x_{1:t})$ is calculated using Bayes' theorem given the monitored positions, x_1, x_2, $\cdots$, x_t $:= x_{1:t}$, up to time t as follows:

$$P(\theta_\eta|x_{1:t}) \propto P(x_t|x_{t-1},\theta_\eta) \times P(\theta_\eta|x_{1:t-1}), \quad (5)$$

where $P(x_t|x_{t-1},\theta_\eta)$ is the likelihood of monitoring and derived directly from Eq. (3). $P(\theta_\eta|x_{1:t-1})$ is recursively updated as the previous posterior.

Given a destination cell, $\theta_\eta \in \Theta$, the moving probability of a target from x_t to X_{t+1} is calculated within the χ^+ from Eq. (3) and Eq. (4). This calculation process is repeated for all the candidate cells, Θ. In each cell within χ^+, the moving probability is calculated depending on the number of candidate cells. After the calculation for all the candidate cells, the moving probability in each cell is averaged. For the averaged moving probabilities, a cell with the maximum probability is estimated as the next position of the target, $\hat{x}_{t+1}$. **Fig. 6** illustrates the calculation process.

In Fig. 6(a), the target is shown by a black dot. The current position is x_t. The set of cells surrounded by the thick line is χ^+. Each of the cells, X_{t+1}, is reachable from the current position, x_t in one step. For these cells, the moving probabilities are calculated as shown in Fig. 6(b). Highly colored cells have higher probabilities. As an example, the cell with a red dot has the maximum probability. Thus the cell is an estimated next position of the target, $\hat{x}_{t+1}$.

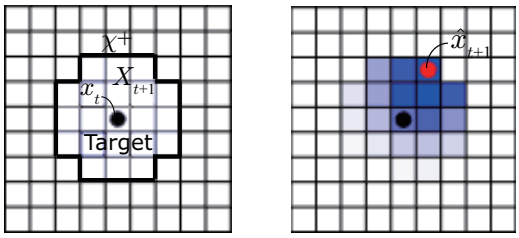

(a)Next cells X_{t+1} in χ^+ (b)Cells with moving probabilities

Fig. 6 Calculation of moving probability

On the basis of the estimated position, $\hat{x}_{t+1}$, the next position, $\hat{x}_{t+2}$, is further estimated. Hence, by repeating the calculation described above, the future positions, $\hat{x}_{t+1}$, $\hat{x}_{t+2}$, $\cdots$, of the target are gradually estimated. Finally, the target reaches a candidate cell. Therefore, a series of the positions, $\hat{x} = \{\hat{x}_{t+1}, \hat{x}_{t+2}, \cdots\}$, is the estimated future positions of the target at time t. **Fig. 7** illustrates the estimated future positions based on the moving probability.

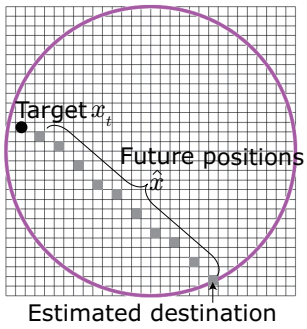

Fig. 7 Estimated future positions of target $\hat{x}$

At time t, the target position is x_t. For the current position, the calculation is repeated until the target reaches a candidate cell. A gray cell has the maximum probability in each calculation. Therefore, the series of the cells is the estimated future positions, $\hat{x}$. Moreover, when the estimated future position reaches a candidate cell, the cell is the estimated destination.

The estimation result described above is for the target in x_t. After the target moved to x_{t+1} in the next time step $t+1$, the position is monitored and the probability density function of the von Mises distribution is calculated as described in Section 2. Based on the moving direction, the estimation process described in this section is sequentially executed. This enables the surveillance system to estimate the correct future positions even if the target changes the moving direction.

4. APPROACH BEHAVIOR OF SEARCHERS

In terms of surveillance, searchers are required to take into account not only a monitoring spot, but also a series of actions toward the spot. This is the optimal approach behavior of searchers. We have proposed an optimal patrolling strategy for mobile robots [4]. This strategy was

based on a value iteration method [5]. In this paper, therefore, we use the value iteration method for the optimal approach behavior.

A value iteration method has been used for calculating an optimal action at every state in a space divided into finite number of discrete states. The output of this method was a so-called state-action map that converts each state to an action [6]. As illustrated in Fig. 2, the space of the environment is already divided into the cells. Therefore, we also focus on this state-action map.

In the value iteration method, the state is defined as a cell occupied by a searcher, and the action is defined as a moving direction of the searcher in the cell. The optimal action indicating the moving direction in each cell is given to the searchers as the policy. For calculating the policy, the following value function is used:

$$V(s_i) = \sum_{s_j \in S} P(s_j|s_i, a_{i,j}) \times \{R(s_j|s_i, a_{i,j}) + \gamma V(s_j)\}, \quad (6)$$

where s_i and s_j represent cells i and j occupied by a searcher. $a_{i,j}$ represents an action to move j from i. $P(s_j|s_i, a_{i,j})$ is a state transition probability, 0 or 1, from s_i to s_j given action $a_{i,j}$. $R(s_j|s_i, a_{i,j})$ is a reward function and γ is a discount factor.

By repeating the recursive calculation of the value function, finally, the state value is optimized on the basis of Bellman update [7]. For the optimal value function, $V^* = \max_{a_{i,j} \in A_i} V$, an optimal action in each state is obtained with the use of the greedy algorithm. The optimal action in state s is represented by $\pi^*(s)$. This policy π^* is used by the searchers as the state-action map. Consequently, the searchers are enabled to move toward a cell with the maximum value of V^* according to the moving direction, i.e., π^*. A series of the actions is the optimal approach behavior of searchers toward the target.

In the surveillance system, the searcher in a cell is allowed to move to the adjacent cells. Hence, the finite action set is defined as $A =$ {front, front right, right, back right, back, back left, left, front left}. **Fig. 8** illustrates an example of V^* and π^*.

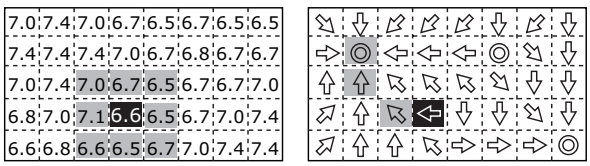

(a)Optimized value function V^* (b)Optimal policy π^*

Fig. 8 Optimal approach behavior

In Fig. 8(a), at the black cell in which $V^*(s) = 6.6$, the greedy algorithm simply selects a cell with the highest state value from the eight adjacent gray cells in addition to the current cell. In Fig. 8(b), $\pi^*(s)$ indicates the moving direction by an arrow. A double circle represents a monitoring spot, which is the end of the approach. Thus the optimal approach behavior of a searcher at the black cell is composed of the following actions: "left," "front left," and "front," as depicted by the gray cells. $\pi^*(s)$ enables searchers to optimally approach the target not only in the black cell, but also in other cells.

As can be seen in Eq. (6), the optimal approach behavior depends on the reward function. In this paper, we present the following reward function:

$$R(s_j|s_i, a_{i,j}) = \omega_1 P(i) + \omega_2 \left(1 - \frac{D_{p_{\max}}(i)}{M}\right) + \omega_3 \left(1 - \frac{D_d(i)}{M}\right), \quad (7)$$

where $P(i) = \frac{p(i)}{p_{\max}}$. $p(i)$ represents a moving probability of cell i, and $p_{\max}$ represents the maximum moving probability defined as $p_{\max} = \max_i p(i)$. $D_{p_{\max}}(i)$ and $D_d(i)$ are normalized distances by M. M is a diameter of the monitoring area. $D_{p_{\max}}(i)$ represents a distance between a cell with the maximum moving probability and i, and $D_d(i)$ represents a distance between an estimated destination cell and i. ω_1, ω_2, and ω_3 are weights.

The reward function in Eq. (7) enables the searcher to proactively approach the target in consideration of the moving probability and destination. In this paper, we further take into account an encounter area between the searcher and target. The encounter area is defined by two circular areas of the searcher and target. A radius of each circle is calculated from the velocity and time. Thus the overlapped area of the two circles is the encounter area. **Fig. 9** illustrates the encounter areas.

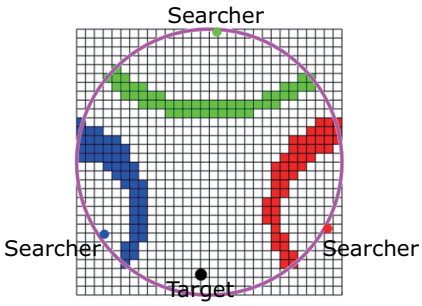

Fig. 9 Encounter areas between three searchers and target

The black dot indicates the moving target. The other three, red, green, and blue dots indicate the searchers. As an example, it is assumed that the target moves with twice the velocity of the searchers. Between the target and each of the three searchers, cells corresponding to the encounter areas are painted in the same colors. In this paper, we present the following reward function:

$$R(s_j|s_i, a_{i,j}) = \alpha(i)\left(\omega_1 P(i) + \omega_2 \left(1 - \frac{D_{p_{\max}}(i)}{M}\right) + \omega_3 \left(1 - \frac{D_d(i)}{M}\right)\right), \quad (8)$$

where $\alpha(i) = 1$ if cell i is in the encounter area; otherwise, $\alpha(i) = 0$.

The reward function in Eq. (8) enables the searchers to approach the target in consideration of the encounter area in addition to the moving probability and destination. In other words, even if a cell has a higher moving probability

or is estimated as a destination, the cells in another area are all ignored.

5. SIMULATION EXPERIMENT

5.1. Estimation Accuracy

5.1.1. Simulation Settings

In this experiment, an incoming target moves toward a destination cell. For this moving target, the future positions are estimated in each simulation step. For the estimation, α used in Eq. (3) is given as $\alpha = 0.5$. In order to discuss the estimation accuracy, we focus on a gap between the estimated destination and true destination. **Fig. 10** shows two moving paths of the target.

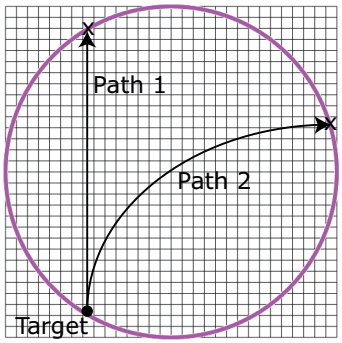

Fig. 10 Straight path (Path 1) and curved path (Path 2)

The target depicted by a black dot is coming into the monitoring area. The radius of the monitoring area is 300 [m]. The target has two destinations marked by "x" and moves along the straight and curved paths. For comparison, the destination is estimated from the most resent monitored positions, x_t and x_{t-1}. A linear path that passes through x_t and x_{t-1} is applied, and the point of intersection between the linear path and the edge of the monitoring area is the estimated destination of the target.

5.1.2. Estimation Results

For the moving target in Fig. 10, two destinations are estimated with the use of the proposed method and comparison method based on a linear path. **Fig. 11** shows the moving probability of the target.

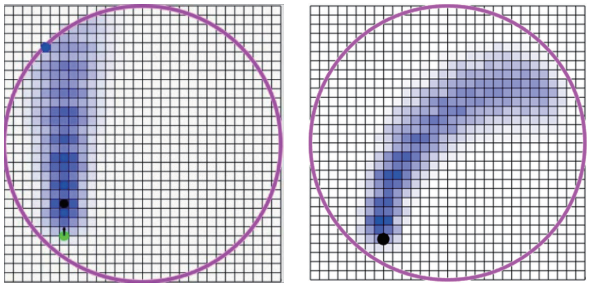

(a)Path 1 (b)Path 2

Fig. 11 Moving probability of target at time t

At time t, the future positions of the target were calculated. The brightness of color in each cell indicates the moving probability. In these results, the moving probabilities of the cells along Path 1 and Path 2 were relatively higher. Although right after the target came into the monitoring area, we can see that the moving direction was predicted successfully. As the estimation result, **Table 1** shows the averaged estimation gap in each step.

Table 1 Estimation gap [m]

	Estimation method	
Path	Linear	Proposed
1	12.9	12.9
2	235.9	32.6

As for Path 1, the estimation gap was 12.9 [m]. Since the size of a cell was 20 [m] $\times$ 20 [m], both the methods successfully estimated the correct destination. As for Path 2, the proposed method estimated the destination with the sevenfold greater accuracy than the comparison method. This is because that the target continuously changed the moving direction rightward. For this target, since the moving direction was correctly predicted as shown in Fig. 11(b), the proposed method succeeded in estimating the destination.

5.2. Surveillance System

5.2.1. Simulation Settings

Fig. 12 illustrates the surveillance environment. The pink circle indicates the monitoring area with a radius of 300 [m].

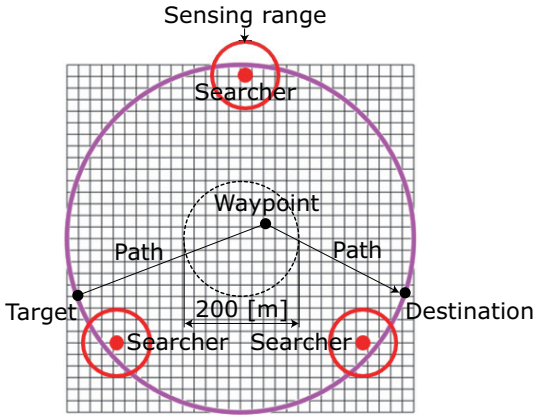

Fig. 12 Surveillance environment

The red dots denote the initial positions of the three searchers. The moving velocity of the searchers is 300 [m/min]. Each searcher is allowed to identify the target in the sensing range depicted by a red circle with a radius of 50 [m]. In total, 1000 trials are conducted. In each trial, one target comes into the monitoring area. At the same time, a waypoint and destination cells are given to the target in a random manner. The waypoint is given within a dashed circle. The destination is given from the candidate cells. The target moves toward the waypoint and destination at a velocity of 600 [m/min].

In order for the searchers to approach the target, three comparison strategies are applied. The first strategy allows the searchers to approach the current position of the target. The second and third strategies are based on the probabilistic approach. The future positions of the target at time t are already estimated as $\hat{x} = \{\hat{x}_{t+1}, \hat{x}_{t+2}, \cdots, \hat{x}_N\}$, where $\hat{x}_N$ corresponds to

the estimated destination. As for the moving probability, a cell of $\hat{x}_{t+1}$ has the maximum probability, $p_{\max}$. Hence, the second strategy allows the searchers to approach the estimated destination, $\hat{x}_N$, and the third strategy allows the searchers to approach a cell with $p_{\max}$, $\hat{x}_{t+1}$. In order for the searchers to optimally approach the target, two more strategies are applied. In the fourth and fifth strategies, Eq. (7) and Eq. (8) are used as the reward function. The weights are given as $\omega_1 = 0.5$, $\omega_2 = 0.2$, and $\omega_3 = 0.3$.

5.2.2. Surveillance Results

In order to evaluate the probabilistic approach of by the searchers, the results of the first, second, and third strategies are compared. **Table 2** shows the number of identified targets for 1000 targets.

Table 2 Number of identified targets

1st: Current position	2nd: $\hat{x}_N$	3rd: $\hat{x}_{t+1}$ with $p_{\max}$
684	703	724

Compared to the first strategy, the searchers based on the second and third strategies identified more targets. This result indicates the effectiveness of estimating the future positions of the target. The third strategy resulted in the best performance from the three strategies. Thus the result of this strategy is compared to the fourth and fifth strategies as shown in **Table 3**.

Table 3 Increased number of identified targets based on optimal approach behavior

3rd: $\hat{x}_{t+1}$ with $p_{\max}$	4th: Eq. (7)	5th: Eq. (8)
724	754	846

Compared to the third strategy, the searchers based on the fourth and fifth strategies identified more targets. This result indicates the effectiveness of optimizing a series of the actions of the searchers. It is noticeable that, although both the fourth and fifth strategies were optimal, the number of identified targets based on the fifth strategy was increased by approximately 100, compared to the fourth strategy. This result indicates the effectiveness of taking the encounter area into account. In other words, the searchers successfully identified the most targets by ignoring the cells outside the encounter areas.

In order to observe the optimal approach behavior of the searchers, their trajectories are compared. **Fig. 13** shows a result in a trial. The trajectories of the searchers are depicted by red, green, and blue lines. The target and the trajectory are depicted by the arrow and black line.

In Fig. 13(a), the trajectory of the moving target reached the destination. This result indicates that the searchers failed to identify the target. In Fig. 13(b), on the other hand, the target was identified by a searcher. These results were caused by the different behavior of the searcher denoted by the red line. The red searcher in Fig. 13(a) first moved in the anterior direction of the target. After that, the searcher changed the direction depending on the target. However, since the target moved with twice the velocity of the searcher, the searcher was left behind

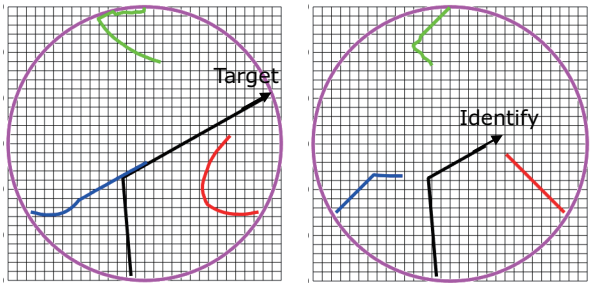

(a)4th: Eq. (7) (b)5th: Eq. (8)

Fig. 13 Comparison of optimal approach behavior

by the target. In contrast, the red searcher in Fig. 13(b) moved almost in the same direction as the target; accordingly, this behavior successfully enabled the searcher to approach and identify the target.

6. CONCLUSIONS

In this paper, we presented an aerial surveillance system composed of single sentinel and multiple searchers. In order for the searchers to identify moving targets, the future positions were estimated and the approach behavior was optimized. In the simulation experiments, the system succeeded in estimating the future positions of a target regardless of the straight and curved moving paths. Furthermore, the searchers based on the optimal approach behavior successfully identified targets as many as possible. Especially, the surveillance performance was increased more than 10 [%] in consideration of the encounter areas between the searchers and target. From these results, finally, the effectiveness of the surveillance system for the moving targets was shown.

REFERENCES

[1] N. Basilico and S. Carpin, "Deploying Teams of Heterogeneous UAVs in Cooperative Two-Level Surveillance Missions," *IEEE/RSJ Int. Conf. on Intelligent Robots and Systems*, pp.610–615, 2015.

[2] G. Best and R. Fitch, "Bayesian Intention Inference for Trajectory Prediction with an Unknown Destination," *IEEE/RSJ Int. Conf. on Intelligent Robots and Systems*, pp.5817–5823, 2015.

[3] S. Hoshino and K. Maki, "Safe and Efficient Motion Planning of Multiple Mobile Robots based on Artificial Potential for Human Behavior and Robot Congestion," *Advanced Robotics*, Vol.29, No.17, pp.1095–1109, 2015.

[4] S. Hoshino *et al.*, "Optimal Patrolling Methodology of Mobile Robot for Unknown Visitors," *Advanced Robotics*, Vol. 30, Issue 16, pp. 1072–1085, 2016.

[5] A.G. Barto and R.S. Sutton, "Reinforcement Learning: An Introduction," MIT Press, 1998.

[6] R. Ueda and T. Arai, "Value Iteration under the Constraint of Vector Quantization for Improving Compressed State-Action Maps," *IEEE Int. Conf. on Robotics and Automation*, pp. 4771–4776, 2004.

[7] R. Bellman, "The Theory of Dynamic Programming," *Bulletin of the American Mathematical Society*, Vol. 60, No. 6, pp. 503–515, 1954.